NRIAG Journal of Astronomy and Geophysics (2016) 5, 147–159

National Research Institute of Astronomy and Geophysics

NRIAG Journal of Astronomy and Geophysics

www.elsevier.com/locate/nrjag

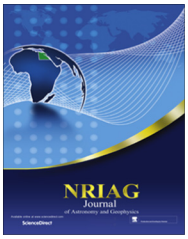

Implementation of ground penetrating radar and electrical resistivity tomography for inspecting the Greco-Roman Necropolis at Kilo 6 of the Golden Mummies Valley, Bahariya Oasis, Egypt

Abbas M. Abbas [a], Hosni H. Ghazala [b], Hany S. Mesbah [a], Magdy A. Atya [a], Ali Radwan [a], Diaa E. Hamed [a,*]

[a] *National Research Institute of Astronomy and Geophysics, 11421 Helwan, Egypt*
[b] *Geology Dept., Mansoura University, Egypt*

Received 7 April 2015; revised 24 January 2016; accepted 24 January 2016
Available online 19 February 2016

KEYWORDS

Archeology;
Bahariya Oasis;
GPR;
ERT;
Golden Mummies

Abstract Bahariya Oasis is one of the lately inspected spots in Egypt and has a long historical record extending from the old kingdom till the emergence of Islam. Since June 1999, the Valley of the Golden Mummies near Bawiti (at kilometer 6 on the road leads to Farafra Oasis) became significant due to the discoveries of amazing mummies of gelded faces. The archeologists believe that the Valley has more valuable tombs that still unrevealed. Also, the possibility that the Greco-Roman Necropolis extends to areas other than Kilo-6 is sustainable.

The ground penetrating radar and electrical resistivity tomography are two geophysical tools that have successful applications in archeological assessment. The two techniques were used in integration plan to assert the archeological potentiality of the studied site and to map the feasible tombs. Sum of 798 GPR profiles and 19 ERT cross sections was carried out over the study area. The results of them were analyzed to envisage these results in archeological terms.

1. Introduction

Bahariya Oasis is a large, oval-shaped NE-oriented depression in the north-central part of the Western Desert of Egypt. It is one of seven major depressions in the Western Desert. It lies between latitudes 27°48′ and 28°30′N, and between longitudes 28°30′ and 29°10′E, at distance of about 300 km southwest of Cairo (Fig. 1). The average depth of the depression from the general desert plateau is less than 100 m (Said, 1962). It has

* Corresponding author.
Peer review under responsibility of National Research Institute of Astronomy and Geophysics.

ELSEVIER Production and hosting by Elsevier

http://dx.doi.org/10.1016/j.nrjag.2016.01.003

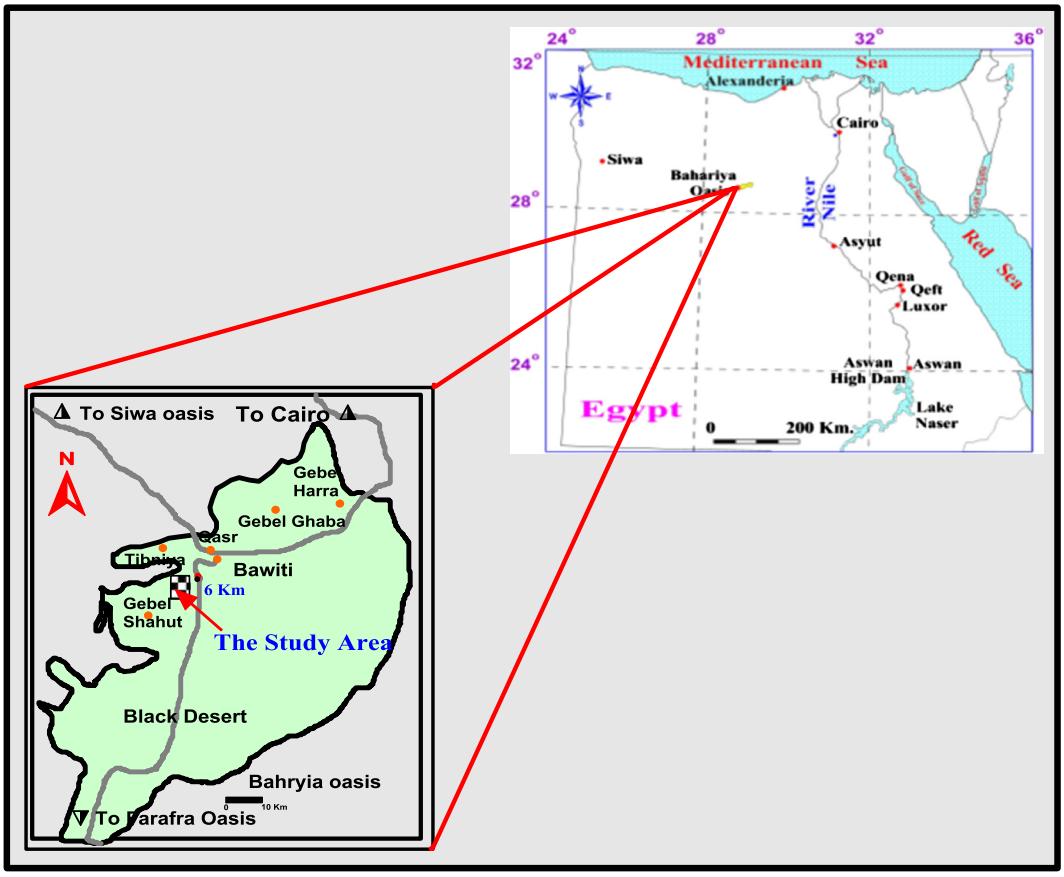

Figure 1 Location map of the study area at Bahariya Oasis.

Figure 2 The shape of one of the reference stations.

a surface area of about 1800 sq. km and is surrounded by plateaus at about 250 m above sea level (Moustafa et al., 2002).

The study area is located in Bahariya Oasis between latitudes 28°19′43.74639″ and 28°19′51.7362″N, and longitudes 28°49′30.01850″ and 28°49′42.8658″E.

The study area is divided into grids in order to apply the geophysical measurements. To allocate the grids in optimum precise, the Global Positioning System "GPS" is used which allows users to determine their location on land, sea, and in the air around the Earth.

The first stage has been to initiate three cement bases to fix three GPS devices (GPS 4000 SSI) on them as reference stations (Fig. 2). These bases are called Bases 1, 2 and 3. To compute the corrected coordinates of these bases accurately, we used the static survey model with interval time 30 s per epoch and left the device working for about 8 h.

The second stage of work was to divide the area under investigation into cells (50 m × 50 m) where we observed every cell uses the Stop and go technique using a very high resolution, an observation per two seconds. The topographic data

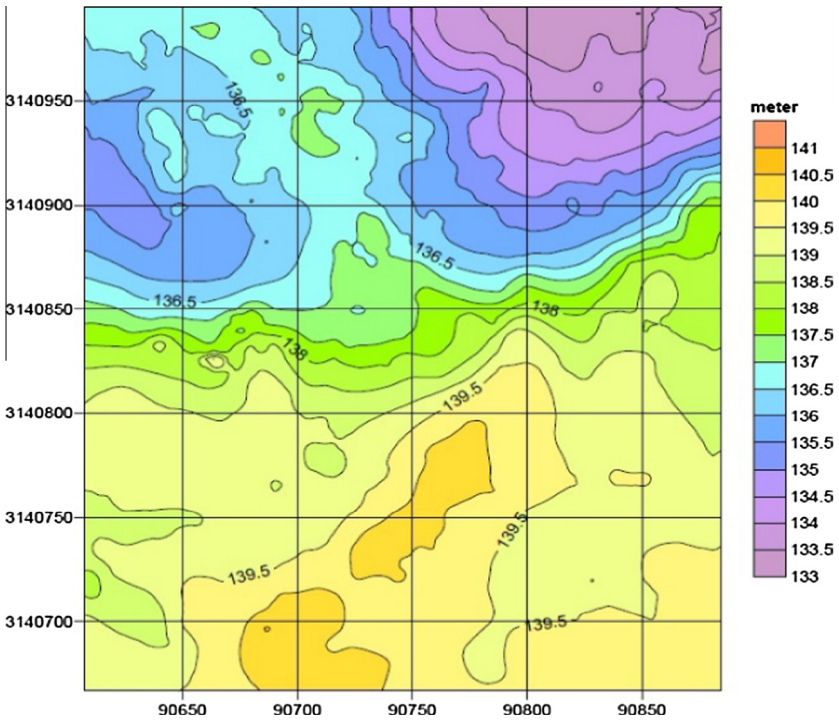

Figure 3 Topographic map of the study area.

were collected using a GPS survey with a very high accuracy reaching less than one centimeter. The collected data were processed using the GPS Processing Program Trimble Business Center (TBC) to get the coordinates of this area, these coordinates are referenced to the Ellipsoid, the projection used was UTM (Universal Transverse Mercator) Zone 36N, the Datum is WGS 84 (World Geodetic System 1984), and the Geoidal Model is EGM96 (Earth Geoidal Model 1996). The main target is to make a topographic map for the study area (Fig. 3).

Bahariya Oasis has several archeological remains, one of them is the Valley of Golden Mummies. This archeological valley holds the largest collection of Egyptian mummies ever found. The present study aims at investigating the potential archeological areas that still unrevealed two geophysical tools: GPR and ERT which are used to verify this aim.

Ground Penetrating Radar (GPR) is commonly used in archeological investigations. It allows the archeologist to cover a wide area in a short period of time, with excellent resolution. It images structures in the ground that are related to changes in dielectric properties. In particular, GPR is well suited to investigate the foundation geometry of archaeological buildings where it is impossible to apply any destructive technique (Abbas et al., 2005).

Electrical Resistivity Tomography (ERT) is an effective tool in archeological investigations as it can show the difference in resistance between air-filled cavities and the surrounding rocks. The air-filled cavity gives high resistivity values compared to the surrounding sandstone which is considered the most outstanding physical feature of a cave (tomb), and for this reason the resistivity method has been the most widely used for cave detection.

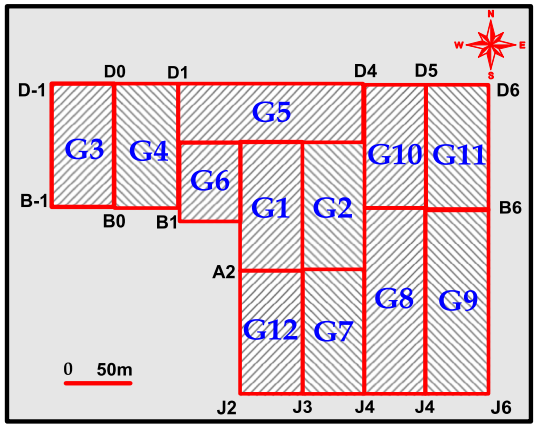

Figure 4 Location map of GPR grids at the study area.

2. Acquisition of GPR and ERT data

The study area that has been surveyed by GPR is subdivided into 12 grids (Fig. 4). The detailed GPR traverses were accomplished on Zig–Zag patterns. SIR 3000 control unit attached to 400 MHz center frequency antennas is used to carry out the detailed archeological prospection to outline the subsurface tombs and archeological features that may present at the study area (Fig. 6a). The total number of profiles measured on the study area is 798.

Nineteen parallel ERT profiles have been conducted at the study area directed from the West to the East. Fig. 5 shows the distribution of ERT profiles at the study area. Syscal-R2

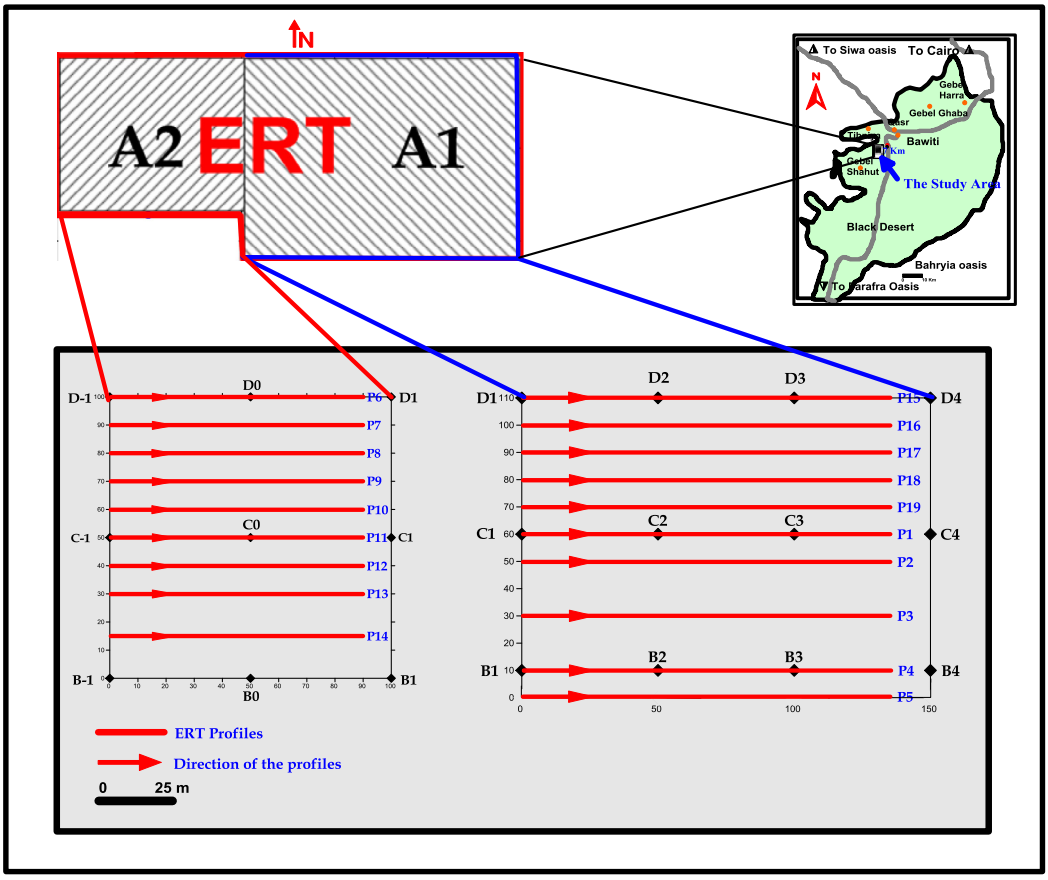

Figure 5 Distribution of ERT profiles at the study area.

(a) **(b)**

Figure 6 (a) Field photograph during the acquisition of GPR profiles, (b) Syscal R2 and multi-electrode system that used during the field survey.

Resistivity meter (IRIS-company, France) and Multi-electrode system with 48 electrodes (Fig. 6b) have been used to carry out the ERT profiles.

Ten parallel profiles P1, P2, P3, P4, P5, P15, P16, P17, P18, and P19 have been carried out at area "A1" of total profile length 141 m and 3 m spacing between the successive electrodes and nine parallel profiles P6, P7, P8, P9, P10, P11, P12, P13, and P14 have been carried out at area "A2" with profile length = 94 m and 2 m spacing between the successive electrodes (see Table 1).

3. Processing of GPR and ERT Data

Although the collected data were generally of good quality, some processing steps were applied using **REFLEX** software, version 6.0 to increase S/N ratio (Abbas et al., 2015).

Table 1 Parameters of the survey GPR grids.

No.	Name of grid	Dimensions of the grid (m)	Number of profiles	Profile length (m)	Profile intervals (m)	Direction of profiles
1	G1	50 × 100	52	50	2	From W to E
2	G2	50 × 100	53	50	2	From W to E
3	G3	50 × 100	101	50	1	From W to E
4	G4	50 × 100	100	50	1	From W to E
5	G5	50 × 150	76	50	2	From S to N
6	G6	50 × 60	32	50	2	From W to E
7	G7	50 × 100	52	50	2	From W to E
8	G8	50 × 150	76	50	2	From W to E
9	G9	50 × 150	76	50	2	From W to E
10	G10	50 × 100	51	50	2	From W to E
11	G11	50 × 100	52	50	2	From W to E
12	G12	50 × 100	51	50	2	From W to E

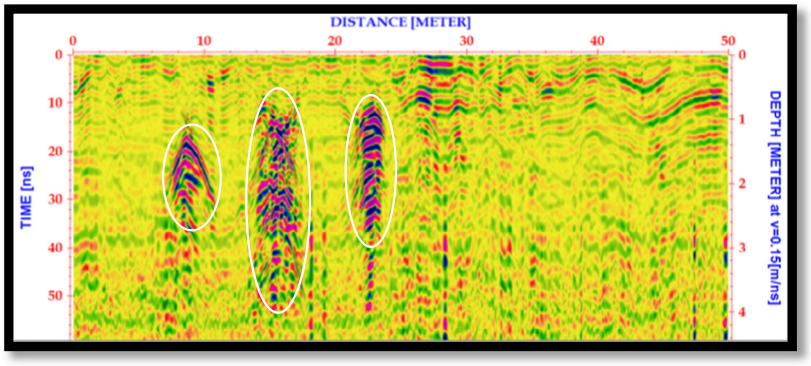

Figure 7 Expected buried features at profile P29.

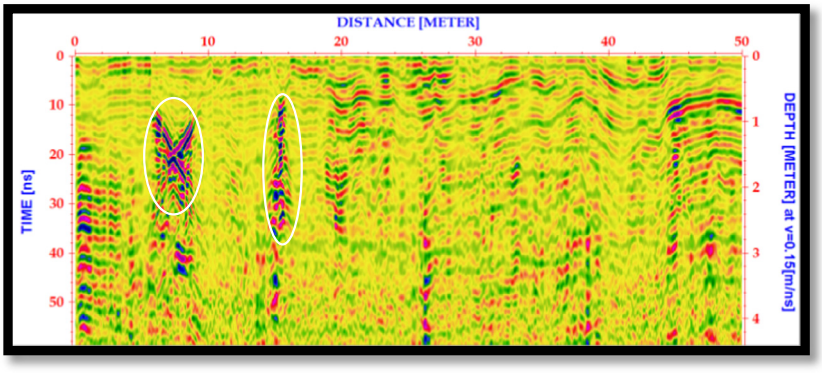

Figure 8 Expected buried features at profile P30.

It is very important after data acquisition to purify the raw data from any noise and unwanted reflections that are produced by antenna "ringing", differences in the coupling of energy with the ground, multiple reflections that occur between the antenna and the ground surface and also background noise (Conyers, 1997), enhance the desired reflections, and correct the horizontal and vertical scales of the raw data. The final steps in data processing involve transforming radar data into usable images. There are certain steps of data processing applied on the raw GPR data using **REFLEX** program. These steps are Static Correction, A band pass filter, Running Average, Background-Removing Filter, Energy decay filter, X Flip the Profile, and Trace Interpol-3D File.

The 2D electrical resistivity data obtained from the field represent the apparent resistivity of the subsurface whereas the true resistivity is required to reflect the best subsurface structures (Loke, 1997). The computer program **RES2DINV** is used to automatically subdivide the subsurface into a number of blocks, and it then uses a least-squares inversion scheme to determine the appropriate resistivity value for each block so

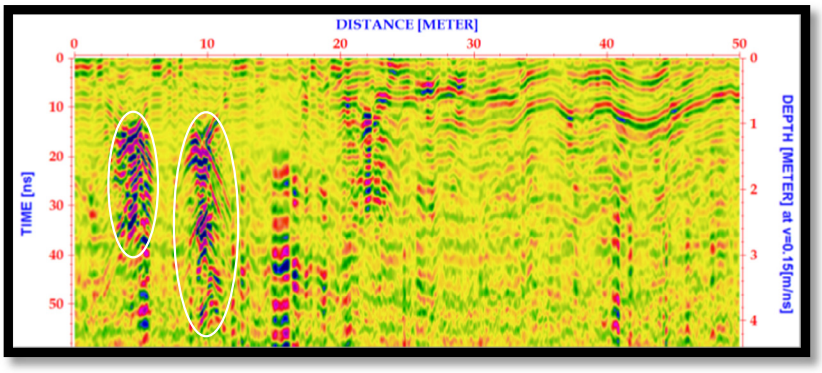

Figure 9 Expected buried features at profile P31.

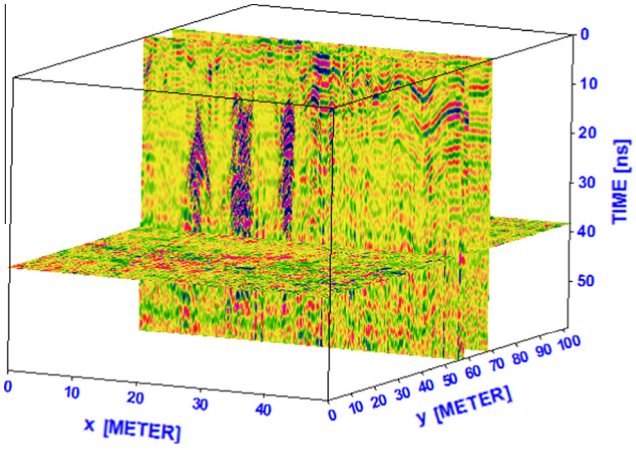

Figure 10 Profiles P29, P30 and P34 in 3D intersect.

Table 2 Summarize the parameters of the detected anomalies along grid G1.

Profile	Object	Surface distance (m)	Depth (m)
P22	1	45	0.8
P29	1	8.7	1.28
	2	15.3	1.17
	3	22.97	0.9
P30	1	7.5	2
	2	15.4	1.3
P31	1	4.77	1.26
	2	9	1.15
P32	1	7.12	0.75
P33	1	15.68	0.85
P34	1	11	1.18
	2	10.78	3.1

that the calculated apparent resistivity values agree with the measured values from the field survey. When the subsurface bodies of interest have gradational boundaries, the conventional smoothness-constrained inversion method (De Groot-Hedlin and Constable, 1990) gives a model which more closely corresponds with reality.

4. Interpretation of GPR and ERT Data

GPR data interpretation is an essential step to determine the location of the anomalies that appears on the processed sections and discriminate them from the other undesired reflections. It also involves tracing the anomalies that appear on the successive sections to determine the subsurface extent and the expected depth of the buried objects that found in the surveyed grids. The results are displayed in three categories: one dimension trace (1D), two dimension cross section (2D) and three dimension block view. In the present study we have achieved the next three procedures on the processed GPR data:

(1) The first step of the interpretation of radar data for each area starts with displaying 2D cross sections that contain the expected buried features.

Table 3 Recognized anomalies at the area "A1".

Profile No.	Recognized archeological anomaly	Horizontal location (m)	Depth (m)	Width (m)	Resistivity range
P1	1	94	1.4	5	High
	2	118	1.4	9	High
P5	1	110	1.4	20	Very high to high
P16	1	32	1.4	26	High
	2	55	1.4	5	Very high
	3	70	1.4	6	High

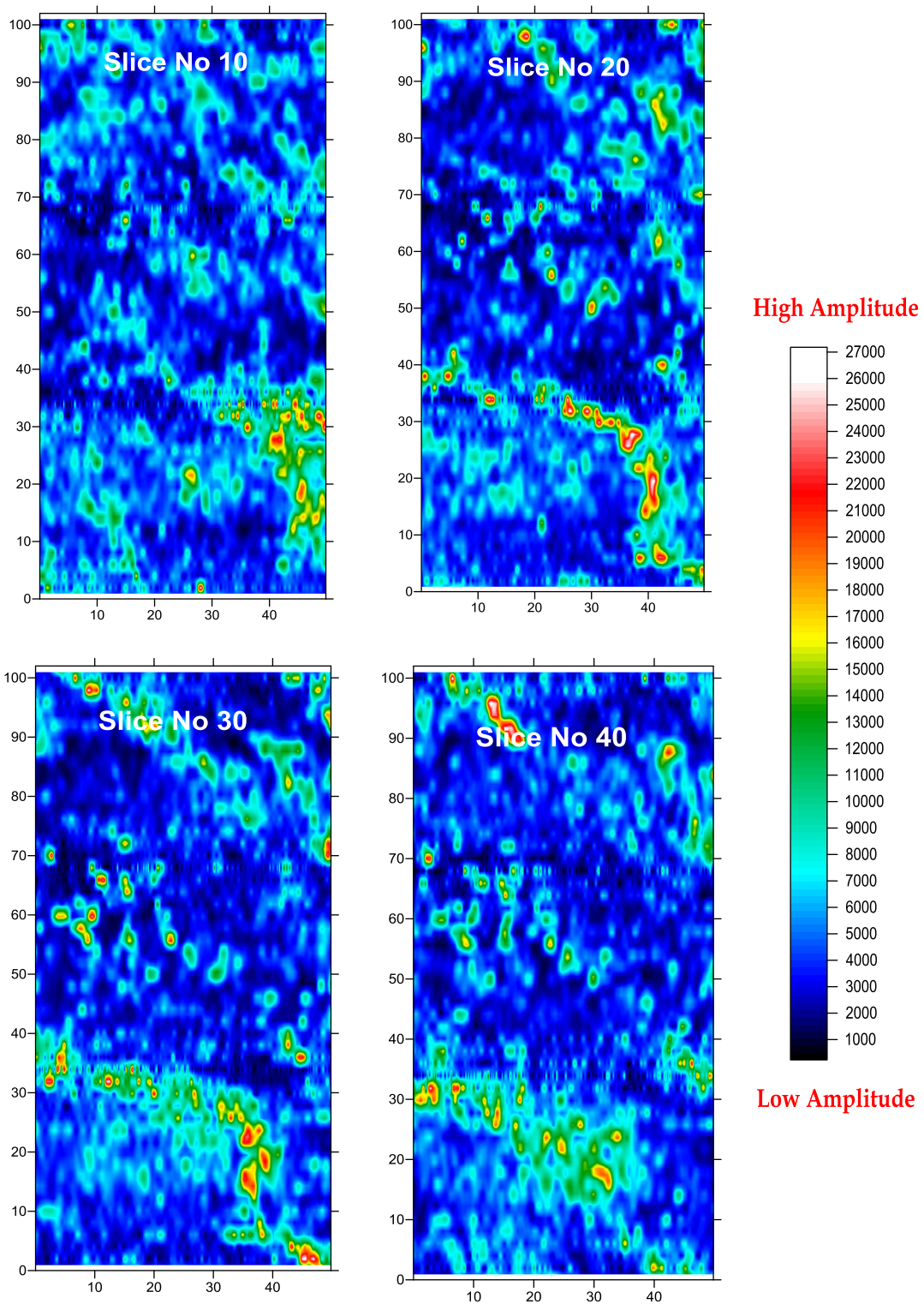

Figure 11 Four time slice maps at 10, 20, 30 and 40 ns.

(2) The second step involves using **REFLEX** program to display 2D profiles in 3D blocks. The profiles may be displayed inside the cube as individual profiles containing obvious features or may be displayed as all in the cube.

(3) The third step is to illustrate four samples of time slice maps then displaying the time slice maps in a continuous series to compare on a single map the location of amplitude anomalies from many horizontal or sub horizontal slices in the ground. In this way the orientation,

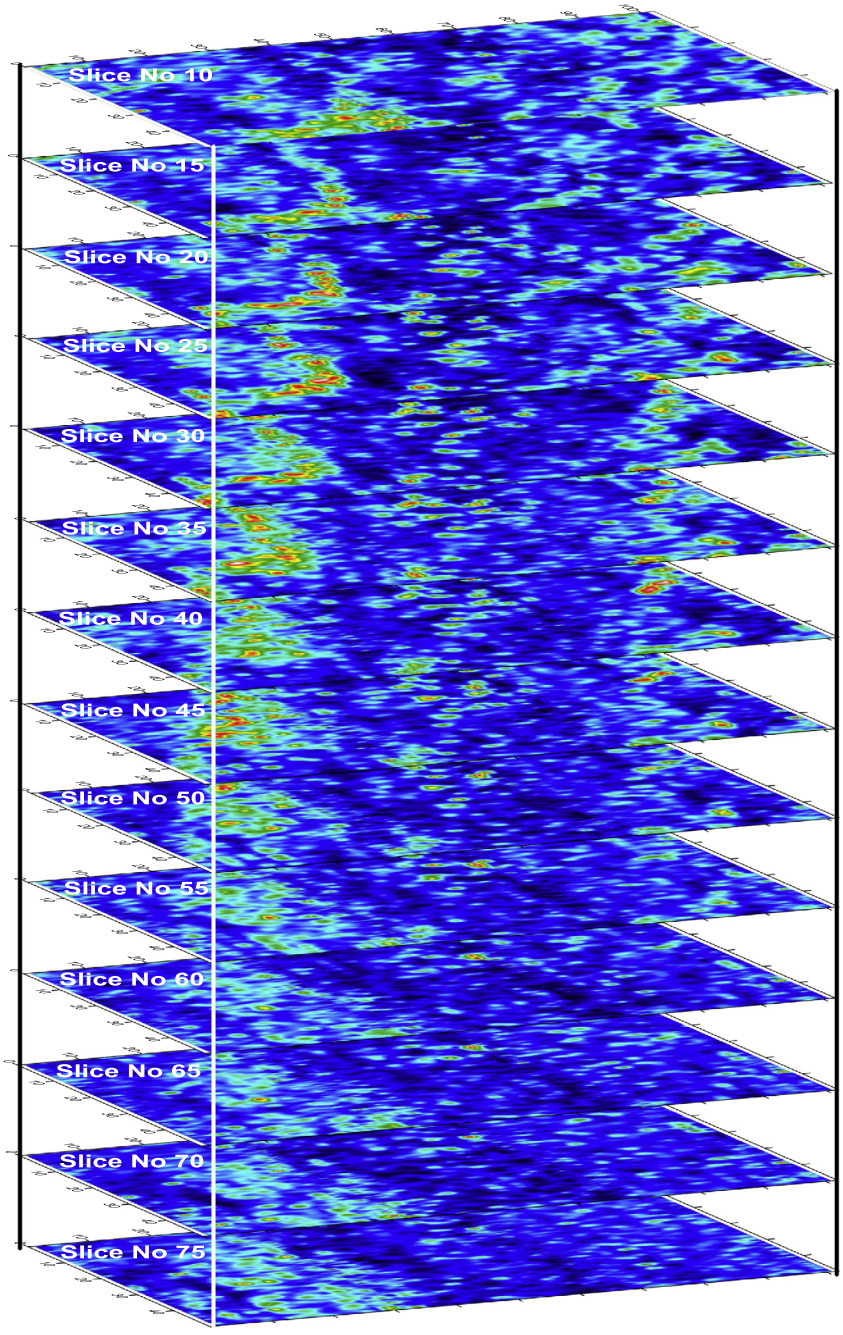

Figure 12 Series of time slice maps from 10 to 75 ns.

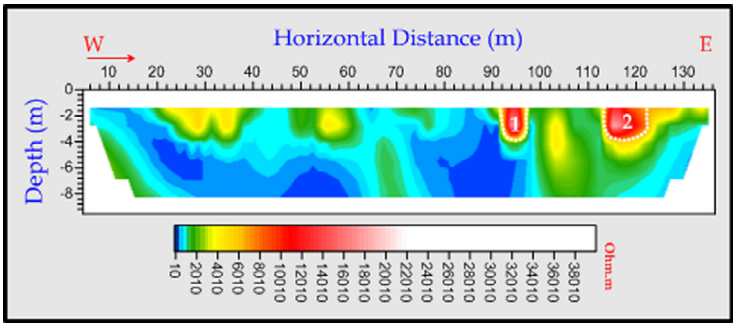

Figure 13 The profile P1 directed from West to East in the area "A1".

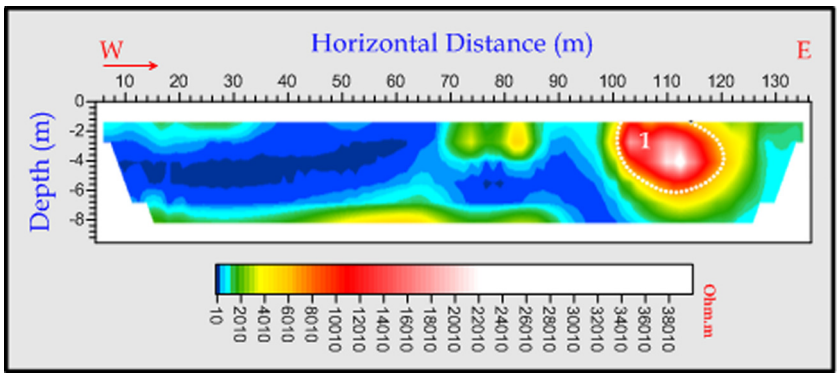

Figure 14 The profile P5 directed from West to East in the area "A1".

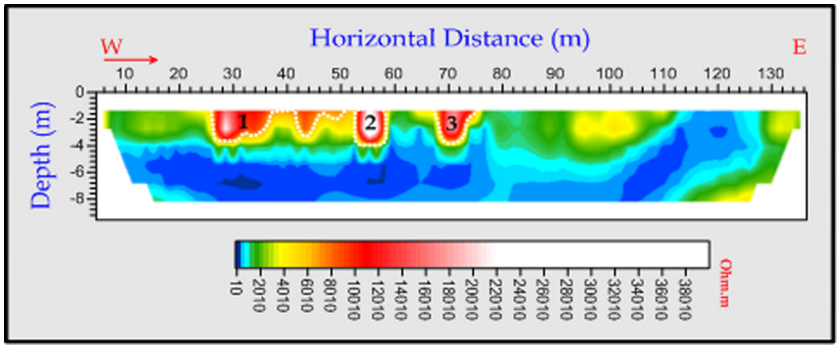

Figure 15 The profile P16 directed from West to East in the area "A1".

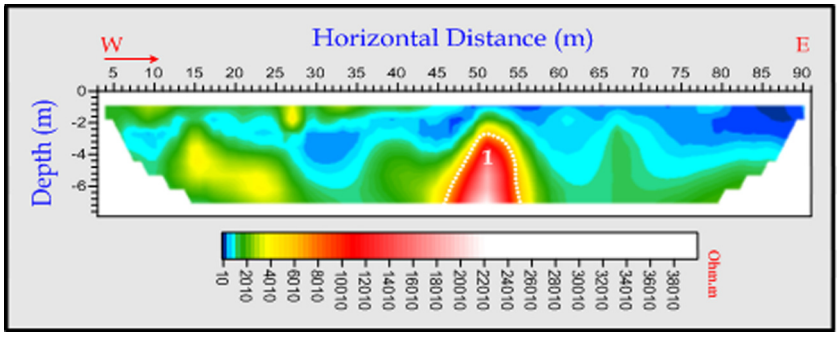

Figure 16 The profile P13 directed from West to East in the area "A2".

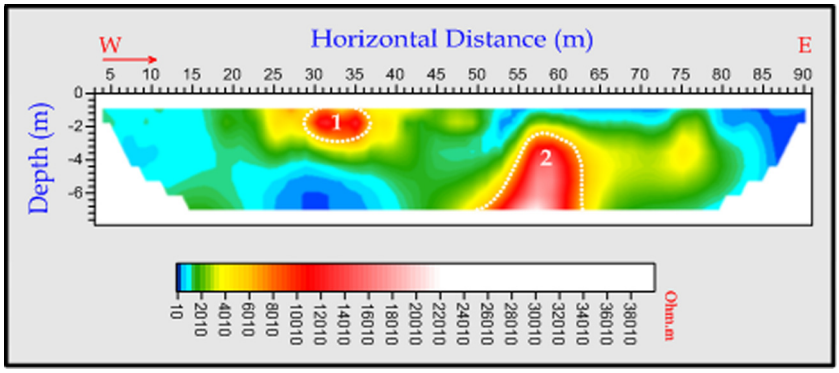

Figure 17 The profile P14 directed from West to East in the area "A2".

Table 4 Recognized anomalies at area "A2".

Profile No.	Recognized archeological anomaly	Horizontal location (m)	Depth (m)	Width (m)	Resistivity range
P13	1	52	2.8	8	High
P14	1	32	1.4	8	High
	2	58	2.4	10	High

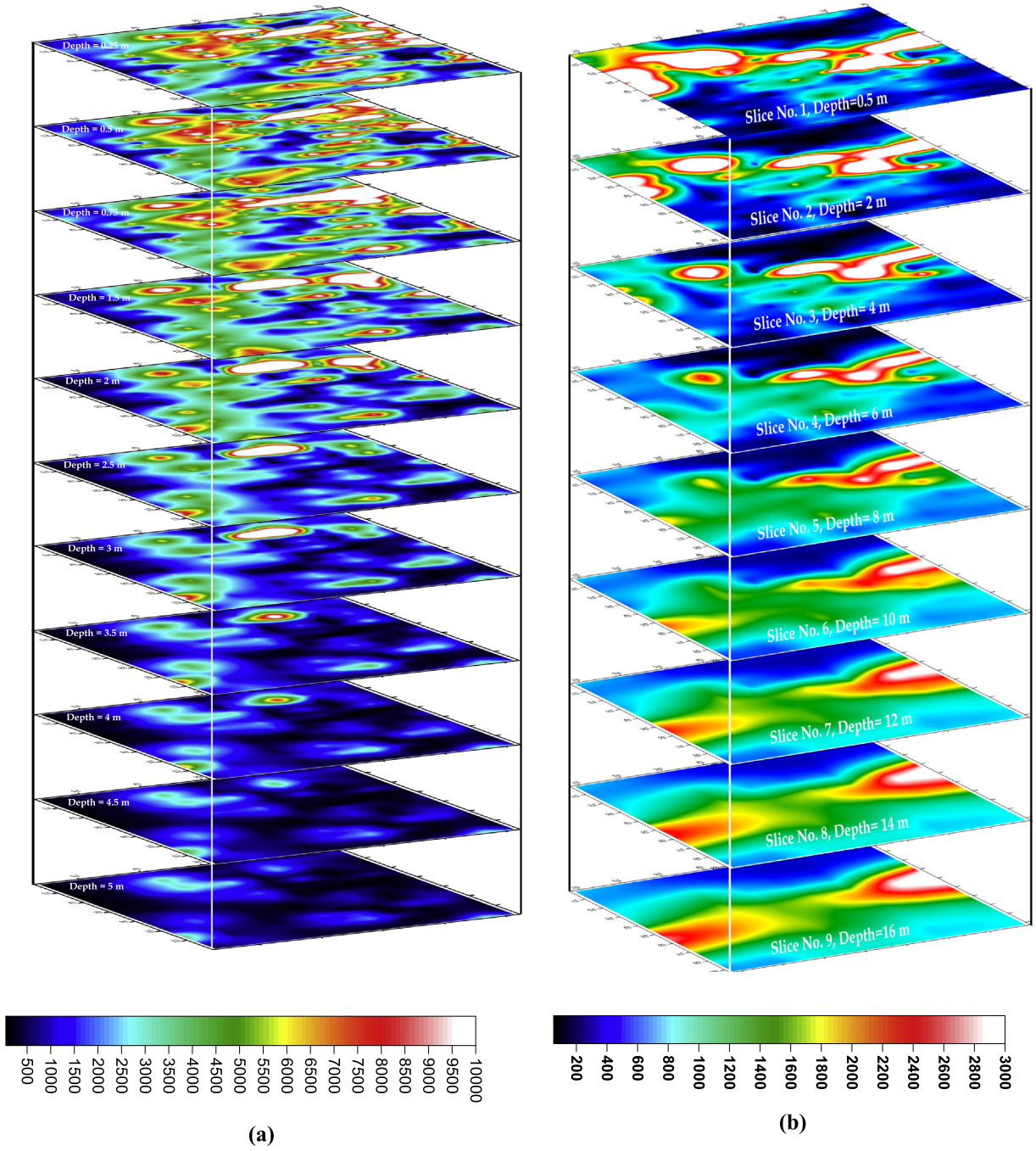

Figure 18 (a) Block of depth slice maps from 0.25 m to 5 m for the area "A1", and (b) Block of depth slice maps from 0.5 m to 16 m for the area "A2".

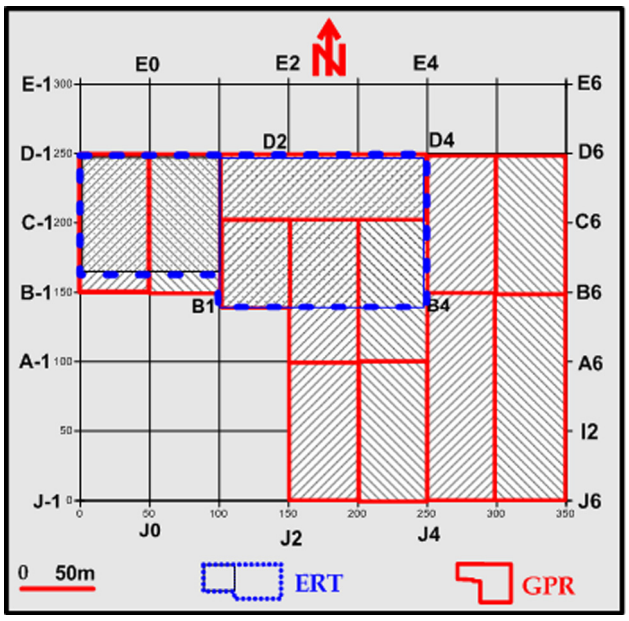

Figure 19 Location map of GPR survey together with ERT survey.

thickness, and relative amplitudes of anomalies are visible in three-dimensions. Amplitude slices are usually made in equal time intervals, with each slice representing an approximate thickness of buried material. The time slice maps are made at each 5 ns for each area.

Grid G1

Some of 2D Sections are illustrated in Figs. 7–9.

The Compiled 3D-intersect of grid G1 is shown in Fig. 10.

Fig. 11 Illustrates sample of the Time Slices of grid G1.

Fig. 12 shows combined map for the time slices of grid G1.

The detected anomalous features are listed in Table 2.

The ERT profiles show areas of very high resistivity values that appeared as white color and high resistivity values that appeared as red color. These values could indicate an empty volume (Open cavity, Shafts, Halls, Rooms, etc.) which in turn could reflect a subsurface archeological potentiality.

Table 3 gathers some of recognized anomalies, their horizontal location, their depth, their width and the resistivity range for each profile of ten profiles covered the area "A1". The 2D profiles are arranged according to the table (Figs. 13–15).

Table 4 lists some of outlined anomalies, their horizontal location, their depth, their width and the resistivity range for each profile of nine profiles covered the area "A2". The 2D profiles are arranged according to the table (Figs. 16 and 17).

5. Electrical resistivity tomography data in 3D

The parallel 2D survey lines for areas A1 and A2 can be combined to 3D maps by using program **RES3DINV**.

The **RES3DINV** program carries out a true 3D inversion (in that the resistivity values are allowed to vary in all three directions simultaneously during the inversion process), whether the data set contains sufficient 3-D information to produce a reasonably accurate 3D model. This program uses the Gauss–Newton method that recalculates the Jacobean matrix of partial derivatives after each iteration (Loke and Dahlin, 2002). The inversion program divides the subsurface into a number of small rectangular prisms, and attempts to determine the resistivity values of the prisms so as to minimize the difference between the calculated and observed apparent resistivity values. The optimization method tries to reduce the difference between the calculated and measured apparent resistivity values by adjusting the resistivity of the model blocks. A measure of this difference is given by the root-mean-squared (RMS) error (Geotomo Software, 2014).

The output of **RES3DINV** Program for the Area "A1" and the area "A2" is exported as *xyz* format and then has drawn on **SURFER 11** (Golden Software, Inc., 2012) program to trace the buried features that found in three dimension in the subsurface.

For the area "A1", the depth of the last slice that resulted from the program is at 25 m, but the lower surface of the expected buried features is appeared till a maximum depth 5 m, so illustration down to depth 5 m was done to concentrate

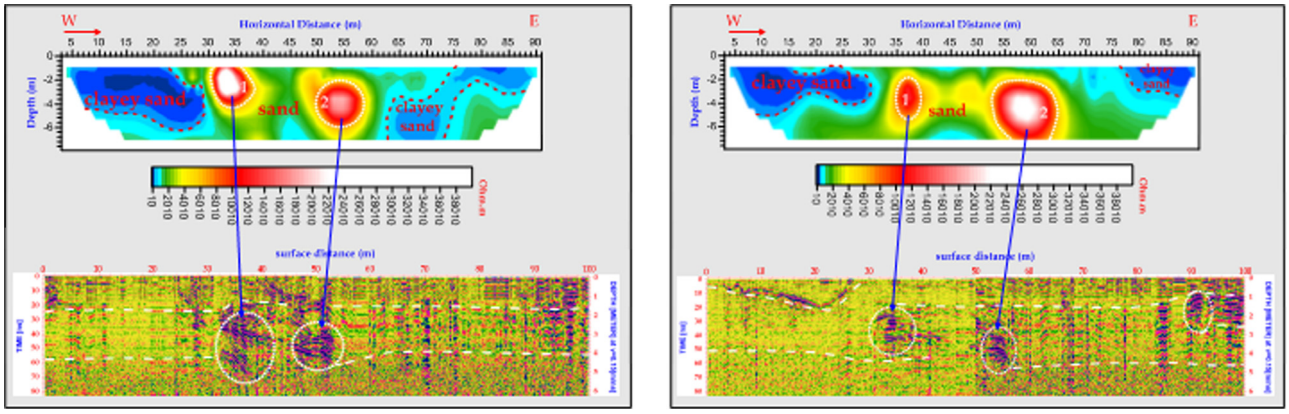

Figure 20 (a) The profile P9 in the area A2 and the radar profiles adjacent to it, and (b) the profile P10 in the area A2 and the radar profiles adjacent to it.

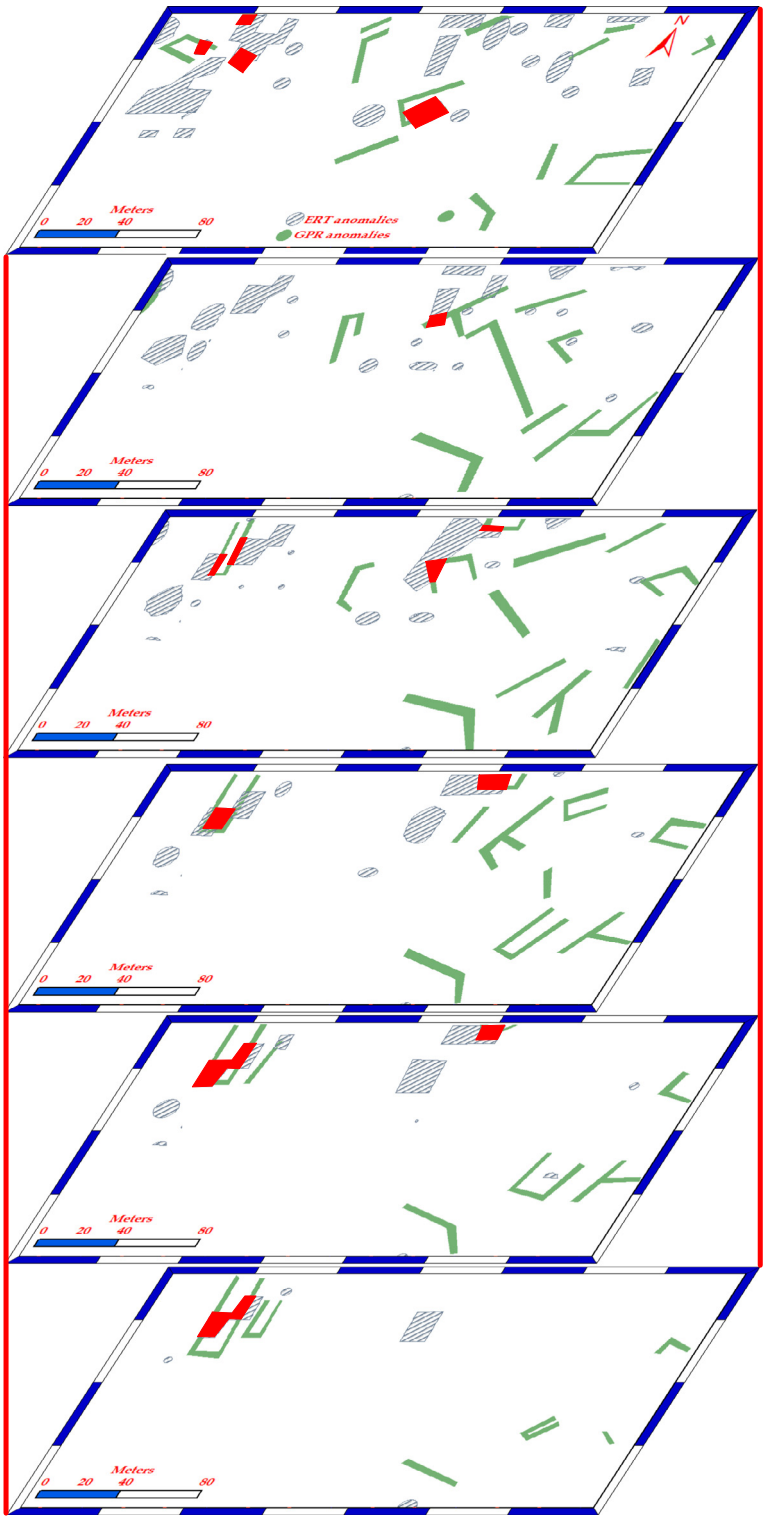

Figure 21 The result of GPR and ERT anomalies at depth from 0.44 m to 2.64 m.

on the anomalous features that may be found in that area at that depth (Fig. 18).

For the area "A2", the depth of the last slice that results from the program is at 16 m and the anomalous features are extended to that mentioned depth, so illustration down to depth 16 m was done to concentrate on the anomalous features that may be found in that area (Fig. 19).

6. Integration between GPR profiles and ERT profiles

The emulation between the outcomes of GPR and ERT requires to exhibit the survey location of these two techniques (Fig. 19).

The following figure illustrates an example of the integration between GPR profiles and corresponding ERT profiles measured at the same line (see Fig. 20).

7. Results of this research

In this research, to integrate the outcomes of the applied two geophysical techniques in one massive result indicating the probable archeological targets, we decided to designate three constrains that are as follows:

- If the two geophysical techniques are affirming the same anomaly, this anomaly is 100% factual archeological structure.
- If the anomaly under investigation was detected due to matching of one technique, then this anomaly is 50% true archeological target.

Fig. 21 illustrates the anomalies that have outlined from both the 3D inversion of ERT profiles and the time-depth slices of the GPR profiles for depth from 0.44 m to 2.64 m.

This figure shows many anomalous features as follows:

- The expected buried anomalies resulted from GPR only are shown in green color. According to the previously assigned constrain, their potentiality of existence is 50%.
- The same due to anomalies resulted from ERT that is shown in dashed lines. According to the above mentioned constrains, their potentiality of existence is 50%.
- The anomalies delineated due to both ERT and GPR are shown in red color and their potentiality of existence is 100%.

References

Abbas, A.M., Kamei, H., Helal, A., Atya, M.A., Shabaan, F.A., 2005. Contribution of geophysics to outlining the foundation structure of the Islamic Museum, Cairo. Egypt. Archaeol. Prospect. 12, 167–176.

Abbas, Abbas M., Salah, Hany., Massoud, Usama., Fouad, Mona., Abdel-Hafez, Mahmoud., 2015. GPR scan assessment at Mekaad Radwan Ottoman – Cairo, Egypt.

Conyers, Lawrence, B., 1997 Ground Penetrating Radar: an introduction for archaeologists/Lawrence B. Conyers and Dean Goodman, pp. 1–232.

De Groot-Hedlin, C., Constable, S., 1990. Occam's inversion to generate smooth, two dimensional models form Magnetotelluric data. Geophysics 55, 1613–1624.

Geotomo Software, 2014. Rapid 3-D Resistivity & IP inversion using the least-squares method (For 3-D surveys using the pole–pole, pole–dipole, dipole–dipole, rectangular, Wenner, Wenner-Schlumberger and non-conventional arrays) On land, aquatic and cross-borehole surveys, 122 p.

Golden Software, Inc., 2012. Surfer for Windows, Version 11, Powerful contouring and Gridding, and 3-D Surfer Mapping.

Loke, M.H., 1997. Electrical imaging surveys for environmental and engineering studies, 63 p.

Loke, M.H., Dahlin, T., 2002. A comparison of the Gauss–Newton and quasi-Newton methods in resistivity imaging inversion. J. Appl. Geophys. 49, 149–162.

Moustafa, Adel R., Saoudi Ati, Moubasher Alaa, Ibrahim Ibrahim M., Molokhia Hesham, Schwartz Bernie, 2002. Structural setting and tectonic evolution of the Bahariya Depression, Western Desert, Egypt, 34 p.

Said, R., 1962. The Geology of Egypt. Elsevier, Amsterdam, 377 p.